04.82.18

Nuclear Engineering and Design 74 (1982) 247-252
North-Holland Publishing Company

SIMULATION OF THE THERMOMECHANICAL EFFECTS ORIGINATED ON A FUEL PIN WITH A CRACKED PELLET BY DIFFERENT POWER RAMP VELOCITIES, USING A TWO DIMENSIONAL FINITE ELEMENT MODEL

Fernando G. BASOMBRÍO *

Institut für Material- und Festkörperforschung III, Kernforschungszentrum Karlsruhe, Karlsruhe, Fed. Rep. Germany

Received 18 October 1982

Thermomechanical effects originated on a fuel pin with a cracked pellet by different power ramp velocities has been studied. To such purpose, the response of a simplified two dimensional finite element model including viscoelastic properties on the pellet and elastoplastic properties on the clad was investigated, under the influence of various ramps with durations ranging from 0 s (instantaneous ramp) to 200 s (slow ramp).

The importance of both, the viscoelastic relaxation effects and their interaction with the plastic behaviour of the clad was put in evidence. It has been observed, that the mechanical response of this fuel pin model strongly depends on the ramp's duration.

Generalities

The present work improves some previous results [6] concerning the thermo-elastoplastic effects of power ramp's velocities on fuel pins, and generalizes them with the inclusion of viscoelastic properties on the UO_2 pellet. It deals with the study of the response of a simplified two dimensional finite element model of a fuel pin with a cracked pellet under the influence of different power ramps. All they range between specific power values χ of 450 and 600 W/cm, with durations from 0 s (instantaneous ramp) to 200 s (very slow ramp).

The model was inspired on typical mechanical situations usually considered on the literature (see for example [1-5]. It is described with some detail in [6] and [7]).

By a "simplified two dimensional model", we understand an idealized interpretation of some of the governing mechanical effects taking place on the real fuel pin (namely the pellet-clad interaction) supported by the following assumptions:

(a) Two dimensional geometric configuration presenting in the pellet six symmetrically displayed opened cracks.
(b) Plane stress.
(c) Small displacements and strains.
(d) Non linear heat conduction.
(e) Von Mises plasticity criterion on the clad (steel). with strain hardening
(f) Linear viscoelastic properties in the pellet (secondary creep). They refer to the properties of the UO_2, for a fixed temperature of 1600 K and an equivalent stress of 600 MPa.
(g) The contact pellet-cladding takes place at a specific power of 450 W/cm. The corresponding steady state was taken as the initial state for all the transient calculations.
(h) Once the contact pellet-clad is reached both, pellet and clad, move solidarily.
(i) The effect on the cladding due to the balance of internal pressure of fission gases and the external coolant pressure, is neglected.
(j) Constant (coolant) temperature of 500°C at the exterior surface of the clad.
(k) Parabolic neutron flux depression.

Assumption (f) is perhaps not very realistic. But taking into account the severe stability restrictions introduced in the creep calculations at high temperatures, additionally magnified by the stress concentrations originated by the cracks, this is in fact an important simplification avoiding the use of implicit algorithms (specially in view of the great amount of calculations here involved).

Assumption (h) was already proved to be very appropriate and a posteriori justified [6]. The remaining assumptions seem to be reasonable [6].

The finite element mesh (see fig. 1) consists on 1600

* On leave of absence from Centro Atómico Bariloche, Comisión Nacional de Energia Atómica—ARGENTINA.

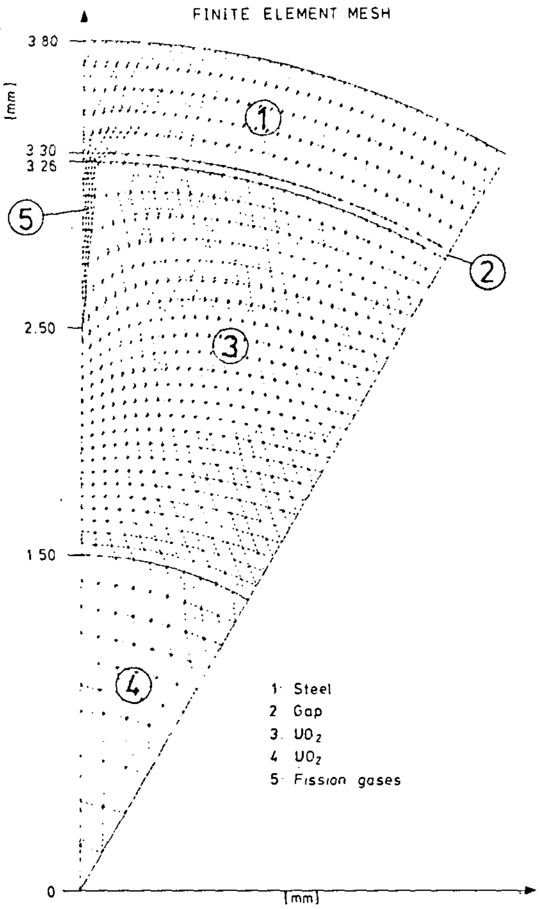

Fig. 1. Finite element mesh and different materials.

Courant's triangular elements and 861 nodes. It was automatically generated with the code REDEF [8], using harmonic transformations. Time steps range between 0.5 s to 5 s.

The non linear transient calculations were performed with the code CTR1 [9,10], and the thermomechanical ones with the code PLASTEF 5, an extension of the thermoplastic finite element codes PLASTEF [11,12] to deal also with viscoleastic effects.

Any other detail concerning the model and its input, as well as many additional bibliographic references should be found on [6] and [7].

2. Basic equations

The underlying system of thermomechanical equations supporting the model is:

Transient heat conduction

$$\rho c(T)\dot{T} - \frac{\partial}{\partial x_j}\left[b(T)\frac{\partial T}{\partial x_j}\right] - q = 0 \qquad (1)$$

(Summation convention of repeated indices is adopted!).

Rate type equilibrium equations

$$\frac{\partial \dot{\sigma}_{ij}}{\partial x_j} = 0. \qquad (2)$$

Compatibility conditions

$$\epsilon_{ij} = \frac{1}{2}\left(\frac{\partial u_i}{\partial x_j} + \frac{\partial u_j}{\partial x_i}\right). \qquad (3)$$

Assumed decomposition of the total strain

$$\epsilon_{ij} = \epsilon_{ij}^{(e)} + \epsilon_{ij}^{(\theta)} + \epsilon_{ij}^{(v)} + \epsilon_{ij}^{(p)}. \qquad (4)$$

Mechanical constitutive equations

$$\epsilon_{ij}^{(e)} = \left(\frac{1}{2G}\delta_{ik}\delta_{jm} - \frac{\nu}{E}\delta_{ij}\delta_{km}\right)\sigma_{km} \ (\textit{Hooke's law}). \qquad (5)$$

$$G = \frac{E}{2(1+\nu)}.$$

$$\epsilon_{ij}^{(\theta)} = \beta T \delta_{ij} \qquad (\textit{thermal dilatation}). \qquad (6)$$

$$\dot{\epsilon}_{ij}^{(v)} = \tfrac{3}{2}\gamma(\bar{\sigma}, T)\frac{\sigma'_{ij}}{\bar{\sigma}} \qquad (\textit{viscoelastic law}). \qquad (7)$$

$\sigma'_{ij} = \sigma_{ij} - \frac{1}{3}\sigma_{kk}\delta_{ij}$ *is the stress deviator.*

$\bar{\sigma} = \sqrt{\frac{3}{2}\sigma'_{ij}\sigma'_{ij}}$ *is the equivalent stress.*

$$\dot{\epsilon}_{ij}^{(p)} = \dot{\lambda}\frac{\partial F}{\partial \sigma_{ij}} \qquad (\textit{plastic flow rule}). \qquad (8)$$

$$F = \bar{\sigma} - H\left(\int \overline{d\epsilon}^{p}\right); \qquad \dot{\lambda} = \frac{\dot{\bar{\sigma}}}{H'}\dot{\bar{\epsilon}}^{p}$$

(*von Mises criterium*)

$\bar{\epsilon}^{p} = \sqrt{\frac{2}{3}\epsilon_{ij}^{(p)}\epsilon_{ij}^{(p)}}$ *is the equivalent plastic strain.*

$\bar{\sigma} = H(\bar{\epsilon}^{p})$

is the equivalent stress/plastic strain curve.

Notation

- $\dot{A}$ time rate of the magnitude A $(=\frac{\partial A}{\partial t})$,
- ρ specific mass,
- c caloric capacity,
- T temperature,
- b heat conduction coefficient,
- q heat generation per unit of volume,

σ_{ij} stress tensor,
ϵ_{ij} strain tensor,
u_i displacement vector,
δ_{ij} Kronecker's tensor,
E Young's module,
ν Poisson's coefficient,
β Thermal dilatation coefficient.

Expressions (1–7) are the complete rate-type equations corresponding to the simplest uncoupled thermoviscoelastic model (see details in [13]). For the present purposes, eq. (7) was particularized to

$$\gamma = k\bar{\sigma}^{n-1} = \mu^{-1}; \quad n = 4.4 \tag{9}$$

with values of $k(T)$ for UO_2 at 1600 K [14] and $\bar{\sigma} = 600$ MPa fixed, as previously mentioned.

3. Description of the results

The geometric two-dimensional configuration of the cracked pellet is represented, for symmetry reasons, as a circular sector of interior angle of 30°. Fig. 1 shows it, indicating the dimensions and the regions corresponding to the different materials. On the straight sides, symmetry boundary conditions are specified. On the curved external side (outer part of the clad) a Dirichlet thermal boundary condition is imposed (coolant's constant temperature of 500°C). Heat generation in the pellet is the only external thermomechanical action. For a given specific power χ at a time t, this axisymmetric heat generation is distributed according to a parabolic neutron flux depression [6]. Each transient calculation (for a given ramp R), is then governed by a linear jump of the specific power χ with a duration of R seconds, between the values

$$450 \text{ W/cm} \leq \chi(t) \leq 600 \text{ W/cm}. \tag{10}$$

On figs. 2 to 5 the thermomechanical responses of the model to various ramps R are exhibited. With the purpose of better evaluating the qualitative and quantitative viscoelastic effects, each ramp was calculated for three different values of the creep coefficient (see eq. (9)): $\gamma = 0$ (no creep); $\gamma = 4.61 \times 10^{-5}$ MPa/s (corresponds to UO_2 at 1600 K and $\bar{\sigma} = 600$ MPa/s [14]) and $\gamma = 1.38 \times 10^{-4}$ MPa/s (three times the previous intensity). For every case, the instant on which the elastic limit is reached is indicated (see figs. 2 and 3).

Fig. 2 comparatively shows the time-dependence of the clad's mean external displacement δ for the different creep intensities. Similarly, fig. 3 refers to the mean contact pressure p_m. For the instantaneous ramp ($R = 0$)

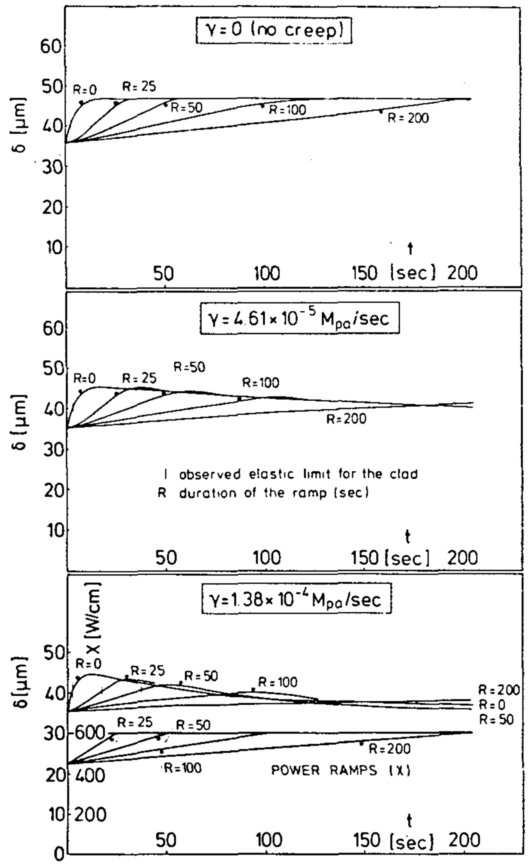

Fig. 2. Mean external displacement (δ) of the clad against time (t) for different ramp durations (R). A comparison for three different values of the pellet's creep intensity ($\gamma = 0$, $\gamma = 4.61 \times 10^{-5}$ and $\gamma = 1.38 \times 10^{-4}$).

and the highest creep coefficient value, we see that at a time of about 190 s the pellet–clad contact is broken ($p_m = 0$). Fig. 4 deals with the pressure p_c at the center of the pellet. Observe that for the non vanishing values of γ an unloading takes place, which in the first instants properly agrees with the relaxation governed by the viscoelastic characteristic time $\tau = \mu/E$ (from the adopted $E_{UO_2} = 130000$ MPa and the three considered values of γ, these are respectively ∞, 16.7 s and 5.57 s).

On fig. 5, the residual mean plastic deformation δ_p is shown for each value of γ, as a function of the ramp duration R. It is defined as the clad's remaining deformation when a monotonical cooling (unloading) is performed, until the ambient temperature is reached. These values were asymptotically estimated substracting from

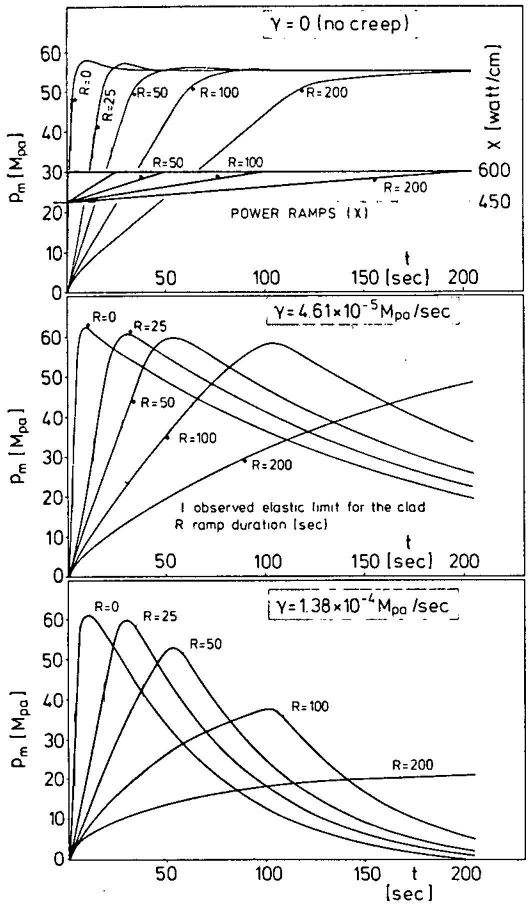

Fig. 3. Mean contact pressure between pellet and clad (p_m) against time (t) for different ramp durations (R). A comparison for three different values of the pellet's creep intensity ($\gamma = 0$, $\gamma = 4.61 \times 10^{-5}$ and $\gamma = 1.38 \times 10^{-4}$).

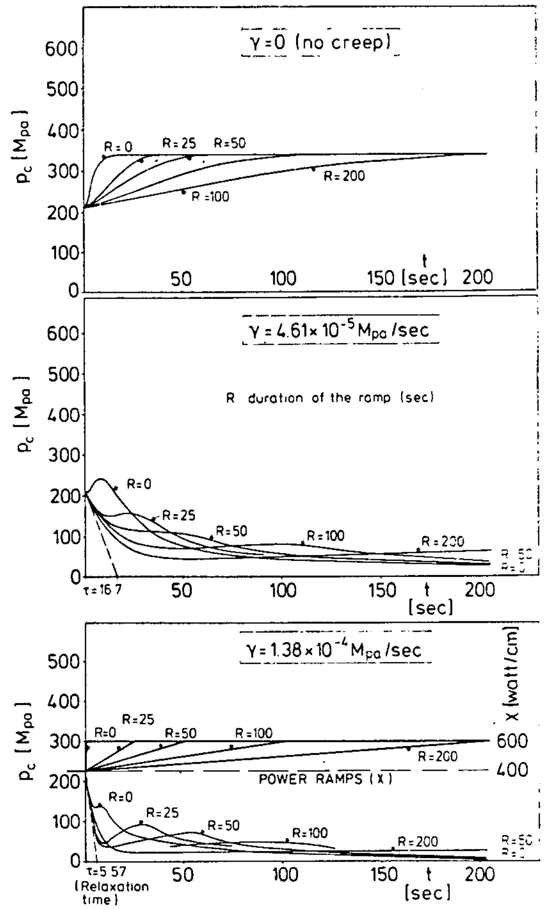

Fig. 4. Pressure at the center of the pellet (p_c) against time (t) for different ramp durations (R). A comparison for three different values of the pellet's creep intensity ($\gamma = 0$, $\gamma = 4.61 \times 10^{-5}$ and $\gamma = 1.38 \times 10^{-4}$).

the displacements δ, the effects of the temperature and the contact pressure p_m.

We conclude this paragraph making some general comments about the precedent calculations. First, it is to be pointed out that by the effects of creep, the strong stress concentration originated by the cracks on the clad [6] (see also fig. 6) essentially disappears. Instead of facing the crack (on the axis $x = 0$, fig. 6), the incipient plastic enclaves take place now in the outer part of the clad, and just in correspondence with the right (inclined) symmetry axis.

For low and vanishing values of the creep's coefficient γ, the clad's plastic collapse state is suddenly reached, leading to some difficulties on the convergence of the algorithms [6]. Typical approximate plastic enclaves are shown on fig 6. For $\gamma = 0$, a collapse state is observed at $t = 75$ s.

On figs. 2 and 3, the unloading on the cladding originated by the creep (relaxation effects) is put in evidence. If from the plotted values one eliminates the time t, the so obtained curves p_m versus δ show the correct elastoplastic loading–unloading aspect. Creep–plasticity interactions are also observed on the behaviour of the maxima of curves p_m vs. t (fig. 3), for increasing creep intensity γ and fixed R. (In the case $\gamma = 0$, no creep, the clad is weakened * by the stress

* That means that in such case p_m reaches at most a value of about the 90% of the theoretical plastic collapse pressure of the clad as a tube.

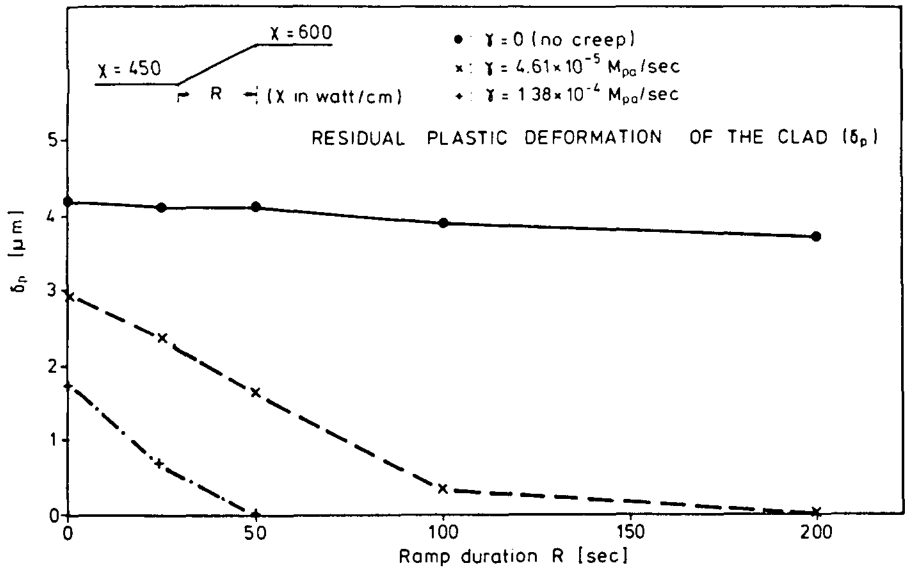

Fig. 5. Estimated residual plastic deformation (δ_p) of the clad as a function of the ramp's duration (R), for different pellet's creep intensities.

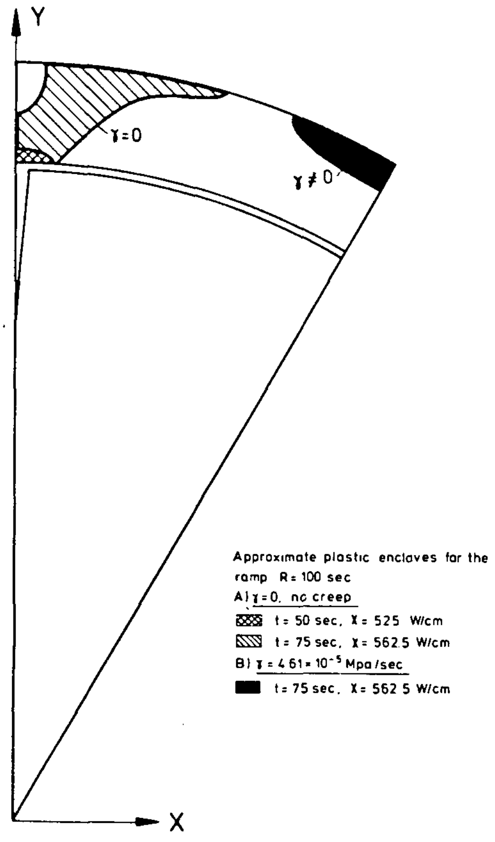

Fig. 6. Typical plastic enclaves for the 100 s ramp.

concentrations produced by the pellet's cracks).

Finally, we point out that still in the absence of creep, a very slight dependence on the ramp velocity is observed (see figs. 3 and 5). This corroborate and improves some previous results [6].

4. Conclusions

The main conclusions of the present study can be briefly summarized as follows:

- For the value of the creep coefficient here considered, the actual results show a strong dependence on the ramp duration. This conclusion is in discrepance with that obtained by Karlsson [4] from a simpler model (assuming *plane strain).*
- In spite of the perhaps not very realistic assumption of linear creep, it has been possible to estimate quantitative (or at least qualitative) viscoelastic effects. They have shown to be of a decisive physical importance. (Note that 1600 K is not a high temperature for a nuclear fuel [6]).
- Mechanical interaction involving creep and plasticity was put in evidence. In this way, a better understanding of the leading mechanical effects on the fuel pin originated by different ramp velocities is possible.
- Fig. 6 insinuates the possibility that in the presence of creep, cracks may propagate from the outer to the

inner face of the clad, instead of the opposite sense (the usually adopted situation) *.

The present results should be supported or otherwise improved by more realistic creep assumptions, investigated at least on simpler models. But of course in such case, many additional complications are to be expected.

Acknowledgements

I remain specially grateful to D. Freund (IMF III/KfK) for proposing me to study the numerical problem of transients on fuel pins; to Dr. K. Lassmann (IRE/KfK) for the orientation received towards the correct statement of the adopted model and for useful suggestions.

I also wish to express my gratitude to Prof. Dr. K. Kummerer (Director of the IMF III) for his hospitality and for providing me all the facilities in the Institute. And finally to the responsibles of the Argentine–German Cooperation Agreement within the frame of which this work was carried out.

References

[1] R.S. Darling, I.B. Fiero and M.E. Scott, Stress distribution in fuel element cladding during pellet–clad interaction, Proc. SMiRT 5, paper D2/8, Berlin (1979).

[2] W. Hering, I.B. Fiero and R.S. Darling, Sensitivity of power ramp induced cladding stress and strain concentrations to modelling assumptions, Proc. SMiRT 5, paper D2/4, Berlin (1979).

[3] B.E. Fredriksson and S.G. Rydholm, Mechanical and temperature contact in fuel rod cladding, Proc. SMiRT 4, paper D3/1*, San Francisco (1977).

[4] B.G. Karlsson, Optimal rate of power increase in nuclear fuel pellet behaviour under dynamic conditions, Proc. SMiRT 4, paper C2/4, San Francisco (1977).

[5] M. Nakatsuka, Theoretical and experimental analysis of cladding strain produced by expansion of cracked fuel pellets, Nucl. Engng. and Des. 65 (1981) 197–204.

[6] F.G. Basombrio, Effects of the power ramp velocity on a fuel pin within a two-dimensional simplified thermoelastoplastic model, Primärbericht PSB-Ber. 1537 (Kl. II), Kernforschungszentrum Karlsruhe (KfK) (December 1981).

[7] F.G. Basombrio, Ein vereinfachtes mechanisches Modell um Wirkungen von verschiedenen Leistungsrampen zu studieren, IMFIII/BEM Notiz Nr. 250, KfK (March 1981).

[8] G. Sánchez Sarmiento, REDEF, Un esquema simple para la generación automática de redes de elementos finitos bidimensionales, Report CNEA-NT 16/80, Comisión Nacional de Energía Atómica (CNEA), Argentina (1980).

[9] F.G. Basombrio and B. Cruz, Ecuación cuasiarmónica con derivada temporal. Su resolución por el método de Faedo-Garlekin con elementos finitos (Programas CTR y CTR1), Report CNEA-NT 30/78, Argentina (1978).

[10] F.G. Basombrio and G. Sánchez Sarmiento, Resolución numérica por elementos finitos de problemas no lineales de difusión dependientes del tiempo, Código CRT1, Rev. SIGMA (Chile) 5 (1979) 37–53.

[11] F.G. Basombrio and G. Sánchez Sarmiento, PLASTEF: a code for the numerical simulation of thermoelastoplastic behaviour of materials using the finite element method, Nucl. Engrg. Des. 49 (1978) 231–241.

[12] F.G. Basombrio and G. Sánchez Sarmiento, Numerical experiments in finite element analysis of thermoelastoplastic behaviour of materials. Further developments of the PLASTEF code, Res. Mechanica 1 (1980) 85–99.

[13] F.G. Basombrio, A résumé of the fundamental laws governing the thermomechanical behaviour of viscoelastic rate-type materials, Primärbericht PSB-Ber. Nr. 1570 (Kl. II) KfK (June 1982).

[14] W. Ernst and H.J. Ritzhaupt-Kleissl, Vorschlag zum Einbau eines Modells zur Beschreibung des sekundären Kriechens von (U, Pu)-Mischoxid in ein Brennstab-Rechenprogramm, Primärbericht PSB-Ber. Nr. 1413 (Kl. II) KfK (July 1980).

* I am indebted to S. Harriague (Comisión Nacional de Energía Atómica) for this remark.